

⁴⁴A. A. Maradudin, E. W. Montroll, and G. H. Weiss, *Solid State Physics*, Suppl. 3, edited by F. Seitz and D. Turnbull (Academic, New York, 1963), p. 236.

⁴⁵J. DeLaunay, *Solid State Phys.* **2**, 257 (1966).

⁴⁶T. H. K. Barron and M. L. Klein, *Proc. Phys. Soc. (London)* **85**, 533 (1965).

⁴⁷I. J. Zucher and G. Chell, *J. Phys. C* **1**, 1505 (1968).

⁴⁸L. Salter, *Phil. Mag.* **45**, 360 (1965).

⁴⁹J. Grindley and Howard, *Lattice Dynamics*

(Pergamon, New York, 1965), p. 125.

⁵⁰H. A. Egger, M. Gsänger, E. Lüscher, and B. Dorney, *Phys. Letters* **28A**, 433 (1968).

⁵¹D. N. Batchelder, M. F. Collins, B. C. G. Haywood, and G. R. Sidey, *J. Phys. C* **3**, 249 (1970).

⁵²W. B. Daniels, G. Shirane, B. C. Frazer, H. Umebayashi, and J. A. Leake, *Phys. Rev. Letters* **18**, 548 (1967).

⁵³M. Born, *J. Chem. Phys.* **7**, 591 (1939).

Properties of Crystalline Argon, Krypton, and Xenon Based upon the Born and Huang Method of Homogeneous Deformations. II. Equation of State and Melting Lines*

G. E. Jelinek

Sandia Laboratories, Albuquerque, New Mexico 87115

(Received 31 August 1970)

Pressure-volume-temperature relationships of solid argon, krypton, and xenon for a Morse potential calculation are compared to the static data of Stewart and Packard and Swenson. Theoretical melting lines based upon mechanical instability of the crystal lattice are presented. It is concluded that within the context of our model below 2 kbar the stability criteria alone are an adequate consideration in the melting line predictions for solid argon, krypton, and xenon.

I. INTRODUCTION

In an earlier paper¹ (hereafter referred to as Paper I) the author described a stressed harmonic potential model calculation of solid argon, krypton, and xenon. Cubic and quartic stress terms in the crystal Hamiltonian were considered via Born and Huang's (BH) method of homogeneous deformations.² The parameters of a Morse potential (see Table II of Paper I) were determined completely from the 0°K solid-state data by a recursive refinement procedure [Eq. (4) of Paper I]. The purpose of this work is to examine the equation of state of solid argon, krypton, and xenon and compare with the static data (to 20 kbar). A study of properties along the "melting line" is also presented. (The "melting line" is based upon Born's mechanical stability criteria.³)

II. EQUATION OF STATE

For our model of solid argon, krypton, and xenon (see Paper I) the Helmholtz free energy was given as a series expansion in the Lagrangian strain parameters (in this case, $\bar{u}_{11} = \bar{u}_{22} = \bar{u}_{33} = u$, $\bar{u}_{12} = \bar{u}_{13} = \bar{u}_{23} = 0$) by

$$F(V, T) = \Phi(V) + F_S(V_0, T) + \sum_{\alpha} F^{(\alpha\alpha)} u + \frac{1}{2} \sum_{\alpha\beta} F^{(\alpha\alpha)(\beta\beta)} u^2, \quad (1)$$

with

$$\Phi(V) = \Phi(V_0) + (1/3!) \Phi_3(V_0) u^3 + \dots + (1/7!) \Phi_7(V_0) u^7,$$

$$\Phi_n(V_0) = \left(\frac{\partial^n \Phi(V)}{\partial u^n} \right)_{u=0}.$$

The $F^{(\alpha\alpha)}$, $F^{(\alpha\alpha)(\beta\beta)}$ anharmonic coupling coefficients are given by Eq. 43.1 of BH. The pressure (P) for volume (V) or vice versa may be calculated from

$$-P = \left[\left(\frac{\partial F}{\partial V} \right)_{T, u=u(T, P)} \right] = \left[\left(\frac{\partial F}{\partial u} \right) \left(\frac{\partial u}{\partial V} \right) \right]_{u=u(T, P)}, \quad (2)$$

where

$$V = V_0 (1 + 2u)^{3/2}, \quad (3)$$

The static equilibrium volume V_0 (per atom) $= \frac{1}{2} \sqrt{2} a_0^3$. The values of a_0 ($P=0$) are given in Table II of Paper I. The pressure (volume) dependence of all the thermodynamic quantities given in Eq. (17) can be obtained by evaluating Eq. (1) for the $P \neq 0$ strains [see Eq. (2)]. All the coefficients in Eq. (1) are evaluated at the zero-temperature zero-pressure static volume. This means that in the equation-of-state (EOS) calculations no additional time-consuming computations of the $F^{(\alpha\alpha)}$ or $F^{(\alpha\alpha)(\beta\beta)}$ coupling parameters are required. The EOS data herein presented are for the Morse potential parameters of argon, krypton, and xenon given in Table II of Paper I.

Many analytical equations of state have been derived following the development of the theory of the finite strain of elastic solids by Murnaghan.⁴ Some of the more commonly used are those developed by Birch,⁵ Gilvarry,⁶ Anderson,⁷ and MacDonald.⁸ However, it is not within the scope of this paper to analyze the theoretical results in terms of such EOS expressions. At this time, interpretation will be given only in terms of comparisons with the re-

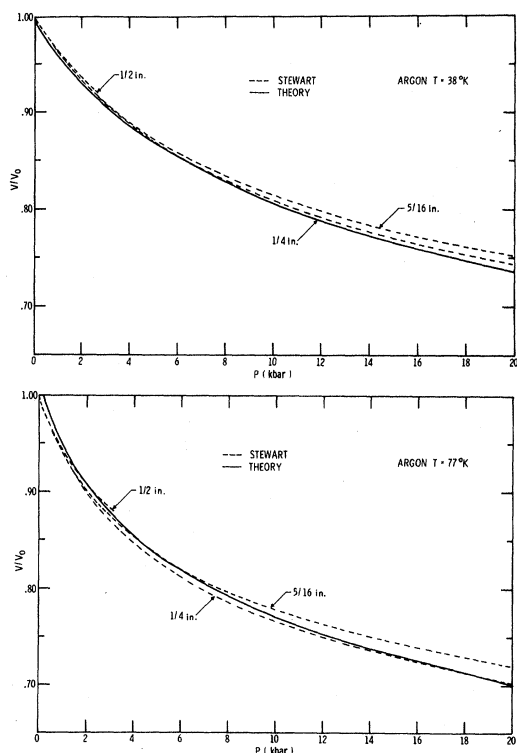


FIG. 1. Isotherms of argon for 38 and 77 °K. Experimental data are from Ref. 9 as observed in sample holders $\frac{1}{2}$, $\frac{5}{16}$, and $\frac{1}{4}$ in. in diameter.

duced data of Stewart⁹ and Packard and Swenson.¹⁰

III. RESULTS OF EOS CALCULATION

In Fig. 1 the 38 and 77 °K isotherms of argon are displayed graphically with the data of Stewart.⁹ Stewart's data are obtained from the three different size sample holders shown in the figure. In order to convert our PV data to the equivalent V/V_0 plot of Stewart, we have taken $V_0 = V(T, P = 0)$ as given by Peterson, Bathchelder, and Simmons.¹¹ In Paper I the excessive dilation for temperatures greater than $\frac{1}{3}T_M$ at zero pressure due to the neglect of truly anharmonic terms was discussed. This effect is visible in the 77 °K isotherm of argon as the pressure goes to zero. Otherwise, the agreement between the calculated and measured isotherms of argon is very good.

The 81 and 115 °K isotherms of krypton are shown in Fig. 2. The agreement is good with the exception of the two smaller sample sizes for pressures less than 10 kbars. The 0 and 150 °K isotherms of xenon are shown in Fig. 3. The experimental data are that of Packard and Swenson.¹⁰ The 0 °K isotherm is an extrapolated isotherm for pressure-volume-temperature data to 20 kbars and from 20 to 160 °K. The theoretical and experimental agreement is excellent with the exception of the excessive expansion at $P = 0$ and $T = 150$ °K. The plus

symbol is the zero-pressure static volume. The volume difference between the point, +, and the curve for $P = 0$ hence is due to the zero-point dilation of the lattice. Packard and Swenson found that the extrapolated P - V isotherm could not be fitted by a theoretical curve based on a Lennard-Jones 6-12 potential. Figure 4 contains a plot of the bulk modulus of argon and krypton as a function of pressure. The plot also contains Stewart's curves (necessarily straight lines) of his data fitted to the Gilvarry⁶ EOS, germane to the low-pressure extrapolation of his pressure-piston displacement curves. Our theoretical curves can be approximated by a low- and a high-temperature linear region with, however, a large change in the slope. The bulk modulus of xenon as a function of the molar volume is plotted in Fig. 4 for 0 and 150 °K. The theoretical calculations of xenon are in excellent agreement with the experimental results, again with the exception of the excess dilation at zero pressure and 150 °K which puts the theoretical curve slightly off the last experimental datum point.

Thus it is observed that while the quasiharmonic theory does not predict the correct temperature derivatives of the Helmholtz free energy for $T > \frac{1}{3}T_M$ (see Paper I), it does obtain nearly correct volume derivatives throughout the temperature range of the

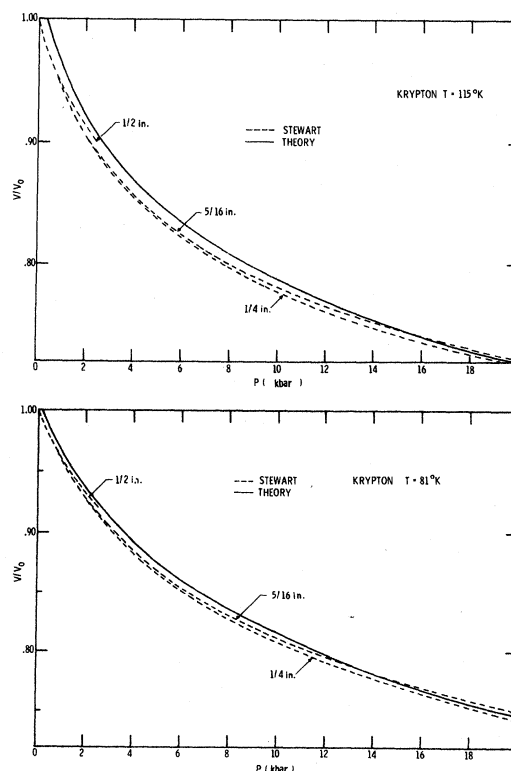


FIG. 2. Isotherms of Krypton for 81 and 115 °K. Experimental data are from Ref. 9 as observed in sample holders $\frac{1}{2}$, $\frac{5}{16}$, and $\frac{1}{4}$ in. in diameter.

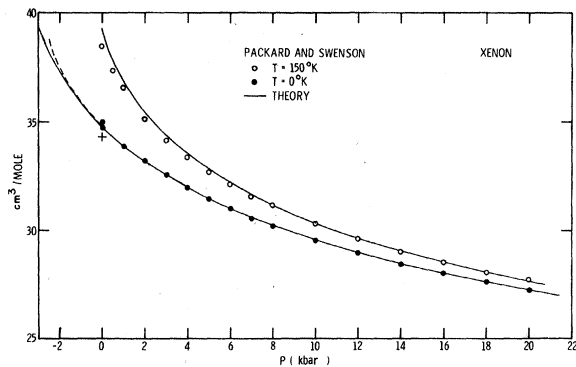


FIG. 3. Isotherms of xenon at 0 and 150 °K. Experimental data are from Ref. 10.

solid. Of course increased pressure is expected to increase the accuracy of the quasiharmonic calculation. These results point to the adequacy of our model for general EOS purposes.

As noted by Holt¹² *et al.*, the thermal contribution is a small percentage of the total elastic constant. Their quasiharmonic lattice dynamical calculations show that an error of 20% in the thermal contribution leads to only 5% error in the elastic constant.

IV. MELTING LINES BASED UPON MECHANICAL INSTABILITY MODEL

Herzfeld and Goepfert-Mayer¹³ and Born,³ by studies of the intermolecular forces of the solid, developed interpretations of the melting process. Herzfeld and Goepfert-Mayer considered the stability of the solid for uniform stresses. The stability limit $(\partial P/\partial V)_T = 0$ for cubic lattices is given by the elastic constants relationship

$$c_{11} + 2c_{12} = 0.$$

Born's investigation included shearing stress limits. The stability criteria for cubic lattices are given by

$$c_{44} > 0, \quad c_{11} - c_{12} > 0, \quad c_{11} + 2c_{12} > 0.$$

Consider the possibilities for instability as the temperature is increased. The case in which the stability against a shearing stress vanishes first ($c_{44} = 0$) would be interpreted as melting. Born suggests describing the state as a gel in which $c_{11} = c_{12}$

TABLE I. Melting point based upon the mechanical instability model.

Solid	$C_{11} = C_{44}$	$C_{11} = C_{12}$	$T_M(P=0)$	$T_M(\text{sat. vapor})$
			Observed (°K) ^a	Observed (°K)
Argon	85.1	90.1	85	83.8
Krypton	115.7	122.4	130	115.9
Xenon	164.1	173.6	170	161.3

^aR. A. Guyer, Solid State Phys. **23**, 413 (1969).

but with a resistance against shearing still occurring ($c_{44} > 0$). For $c_{11} + 2c_{12} = 0$, the lattice is completely unstable and has no cohesion at all.

V. MELTING LINE RESULTS

In our crystal model calculations for a given pressure the temperature dependence of the elastic constants is such that $c_{44} > c_{12}^T$. For our model an ordering of the occurrence of instabilities is

- ① $c_{11}^T = c_{44}$,
- ② $c_{11}^T = c_{12}^T$,
- ③ $c_{11}^T + 2c_{12}^T = 0$.

Our "theoretical melting line" plots are for the condition $c_{11}^T = c_{44}$. Thus, though the onset is one of gel-type characteristics, it can be seen from Table I and Fig. 5 that the complete transition ① → ③ occurs over a narrow temperature range.

These mechanical stability criteria can give only an upper limit to the melting temperature and vol-

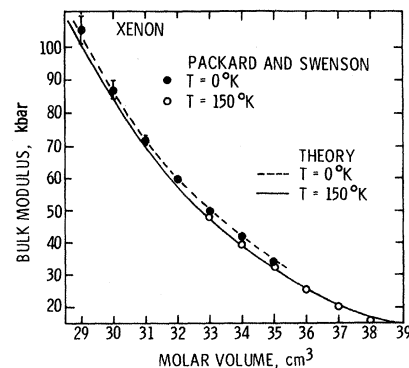
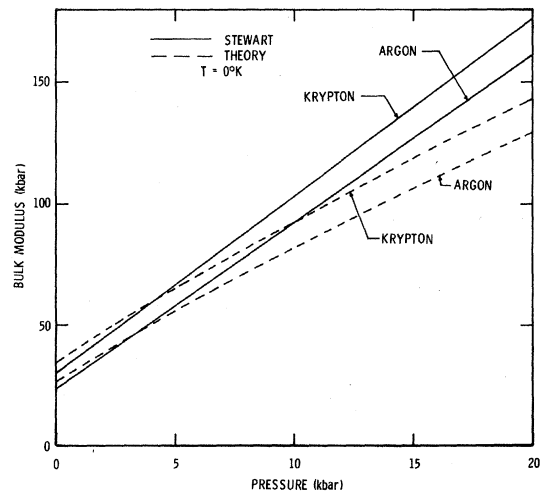


FIG. 4. (a) Pressure dependence of the bulk moduli of argon and krypton at 0 °K; solid curve derived by Stewart for the Gilvarry EOS. (b) Volume dependence of the bulk modulus of xenon for 0 and 150 °K. Experimental data from Ref. 10.

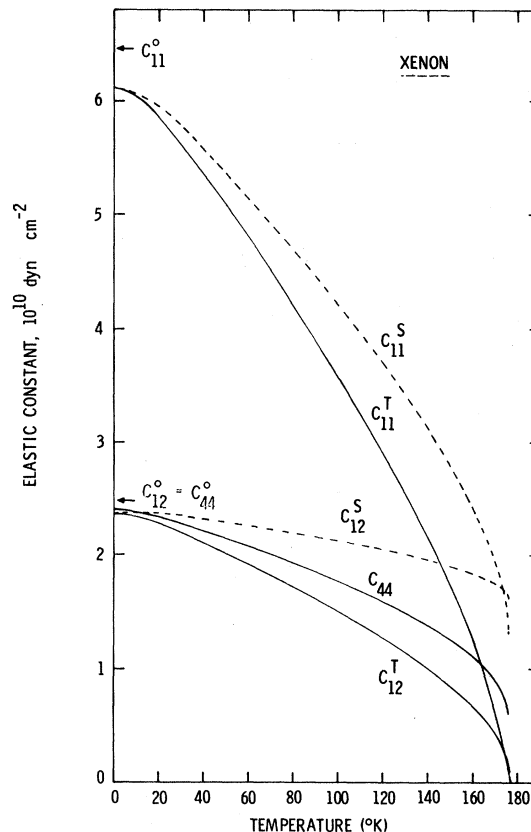
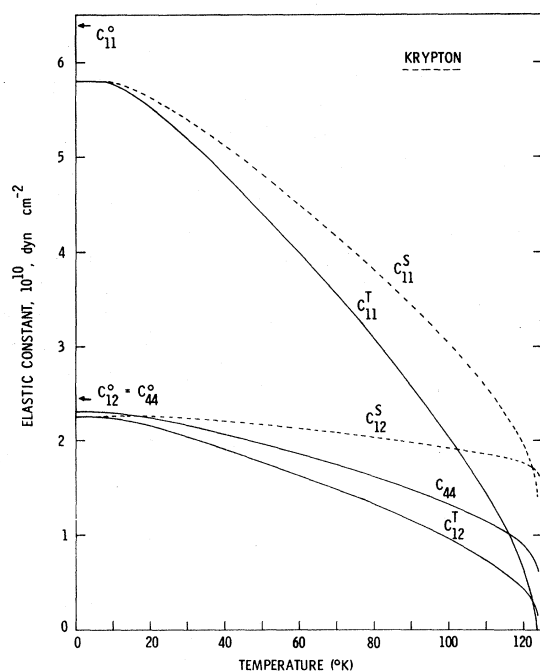
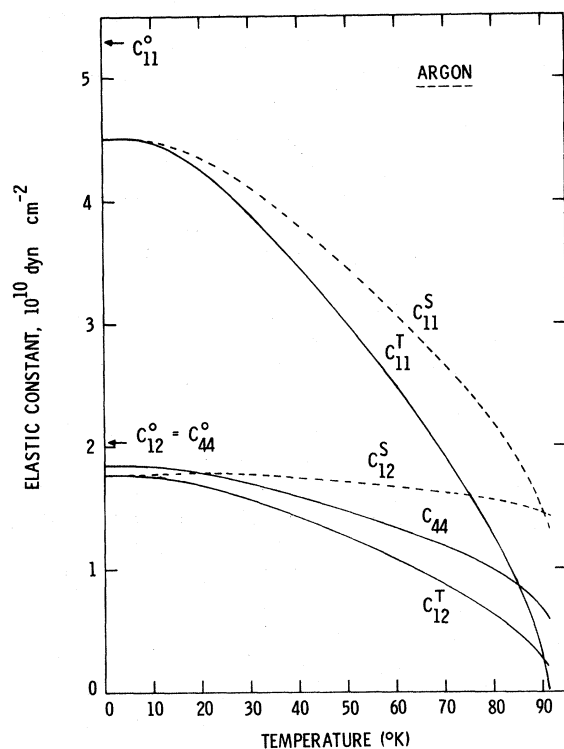


FIG. 5. Adiabatic (C_{ij}^S) and isothermal (C_{ij}^T) elastic constants of argon, krypton, and xenon.

ume.¹⁴ A true theory of the melting phenomenon must be based upon an equivalence of the Gibbs free energy of the solid and liquid models. (This is a bare minimum—there is also the question of the relative importance of order-disorder phenomena¹⁵ in the melting process.)

The chemical potential ($\mu = F + PV$) of our calculations for argon correlates well with the solid

models of Kerber.¹⁶ Hunter and Siegel¹⁷ have shown that, considering the transmission of elastic waves, a crystalline solid behaves as such right up to the melting point. These observations support the identification of the mechanical instability with the solid-liquid transition.

The temperature dependence (for zero pressure) of the isothermal (C_{ij}^T) and adiabatic (C_{ij}^S) elastic

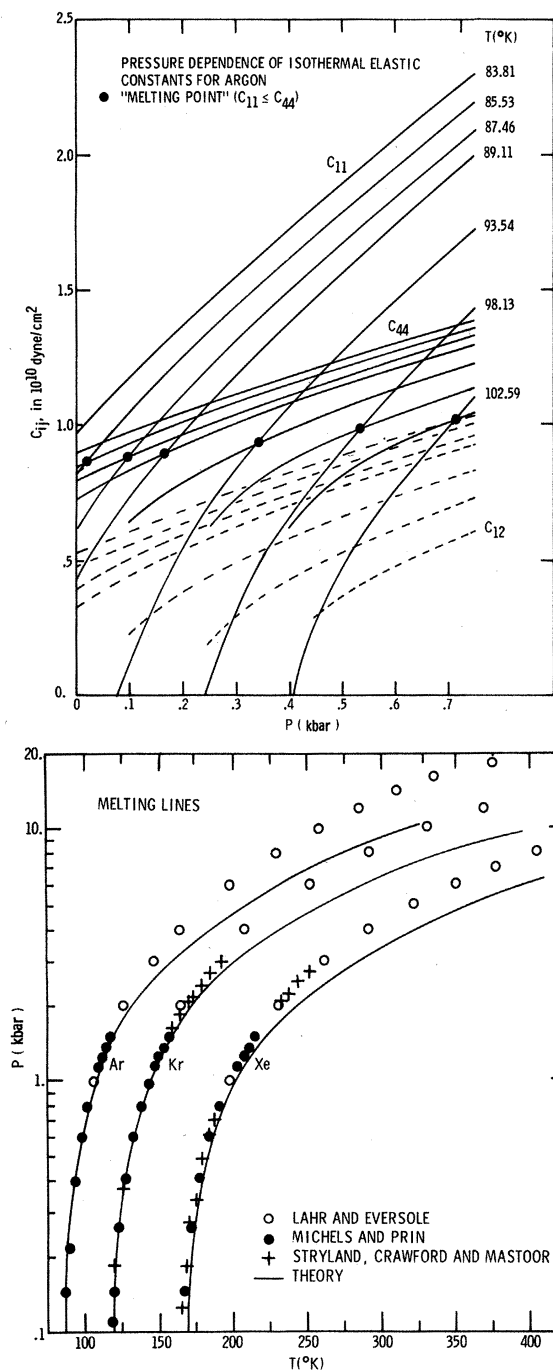


FIG. 6. Melting lines based upon the instability criterion $C_{11}^T = C_{44}^T$. Experimental data are from Ref. 19 (open circles); Ref. 20 (closed circles); and Ref. 21 (+).

constants of argon, krypton, and xenon including the mechanical instability crossover region are shown in Fig. 5. (Qualitatively similar behavior was observed by Ida.¹⁸ Ida's investigation of melting involved the concept of a critical energy for thermal vibration related to "vibrational elongation" caused by the anharmonicity.) The large volume expansi-

vities observed in Paper I coincide with the rapid temperature variation of the isothermal elastic constants at high temperatures, $T > \frac{1}{3}T_M$. The pressure dependence of the elastic constants of argon for a few temperatures is shown in Fig. 6(a). The loci of the points $C_{11} = C_{44}$ are the melting lines shown in Fig. 6(b). For pressures less than 2 kbar the theoretical melting lines of argon, krypton, and xenon are in very good agreement with the experimental melting lines of Lahr and Eversole¹⁹; Michels and Prins²⁰; Stryland, Crawford and Mastoor²¹; and Stishov, Makarenko, Ivanov, and Fedosimov²² (not shown).

In an analysis of the high-pressure data it is pertinent to note the following observations. As opposed to the zero-pressure curve, Fig. 3 of Paper I, the rms displacements along the melting line are a slowing-increasing function with temperature (see Fig. 7). Crawford and Daniels²³ find $[\langle u^2 \rangle / a^2]^{1/2} = 0.098$ at 94 °K and 0.104 at 201 °K for a calculation based on an Einstein model. This is a 6% change for 100 °K temperature change. For our theoretical calculation we obtain 0.093 and 0.097, respectively, for a 4.3% increase in $[\langle u^2 \rangle / a^2]^{1/2}$ along the theoretical melting line.

VI. CONCLUSIONS

In this paper we have presented EOS calculations for solid argon, krypton, and xenon. Our calculations show that even though the quasiharmonic calculation is seriously inadequate for the thermal contributions to the free energy, the strain dependence of the model is quite good. Thus, the elastic constants and bulk modulus (both second-order strain derivatives of the free energy) are in good agreement with experiment. In fact, the quantitative accuracy of the model increases with increasing pressure such that the P - V relationship in the range 5–20 kbar is in good agreement with experiment for

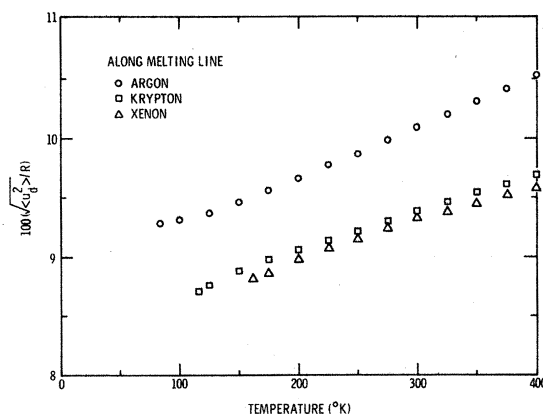


FIG. 7. Temperature dependence of the rms displacement as a percentage of the nearest-neighbor distance along the melting line.

temperatures up to 7, 2, and 11 °K of the zero-pressure melting points of argon, krypton, and xenon, respectively.

As noted above, a true theory of melting must be based upon an equivalence of the Gibbs free energies

of the solid and liquid. Nevertheless, within the context of our calculation the mechanical instability of our model correlated well (below 2 kbar) with the observed melting lines of solid argon, krypton, and xenon.

*Work supported by the U. S. Atomic Energy Commission.

¹G. E. Jelinek, preceding paper, Phys. Rev. B **3** 2716 (1971).

²M. Born and K. Huang, *The Dynamic Theory of Crystal Lattices* (Oxford U., New York, 1954).

³M. Born, J. Chem. Phys. **7**, 591 (1939).

⁴F. D. Murnaghan, *Finite Deformations of an Elastic Solid* (Wiley, New York, 1951).

⁵F. Birch, J. Geophys. Res. **56**, 227 (1952).

⁶J. J. Gilvarry, J. Appl. Phys. **28**, 1253 (1957).

⁷O. L. Anderson, J. Phys. Chem. Solids **27**, 547 (1966).

⁸J. R. MacDonald, Rev. Mod. Phys. **38**, 669 (1966).

⁹J. W. Stewart (private communication); J. Phys. Chem. Solids **29**, 641 (1968).

¹⁰J. R. Packard and C. A. Swenson, J. Phys. Chem. Solids **24**, 1405 (1963).

¹¹O. G. Peterson, D. N. Batchelder, and R. O. Simmons, Phys. Rev. **150**, 703 (1966).

¹²A. C. Holt, W. G. Hoover, S. G. Gray, and D. R.

Shortle, Physica **49**, 61 (1970).

¹³K. F. Herzfeld and M. Goeppert-Mayer, Phys. Rev. **46**, 995 (1934).

¹⁴J. DeBoer, Proc. Roy. Soc. (London) **A215**, 4 (1952).

¹⁵J. E. Lennard-Jones and A. F. Devonshire, Proc. Roy. Soc. (London) **A170**, 464 (1939).

¹⁶R. I. Kerber, J. Chem. Phys. **52**, 2436 (1970).

¹⁷L. Hunter and S. Siegel, Phys. Rev. **61**, 84 (1942).

¹⁸Y. Ida, Phys. Rev. **187**, 951 (1969); Phys. Rev. B **1**, 2488 (1970).

¹⁹P. H. Lahr and W. G. Eversole, J. Chem. Engr. Data, **7**, 42 (1962).

²⁰A. Michels and C. Prins, Physica **28**, 101 (1962).

²¹J. C. Stryland, J. E. Crawford, and M. A. Mastoor, Can. J. Phys. **38**, 1546 (1960).

²²S. M. Stishov, I. N. Makarenko, V. A. Ivanov, and V. I. Fedosimov, Zh. Eksperim. i Teor. Fiz. **11**, 22 (1970) [Sov. Phys. JETP Letters **11**, 13 (1970)].

²³R. K. Crawford and W. B. Daniels, J. Chem. Phys. **50**, 3171 (1969).

Interference in LO-Phonon-Assisted Absorption*

Richard G. Stafford

Department of Physics, University of Oregon, Eugene, Oregon 97403

(Received 31 August 1970)

In this paper we calculate by second-order perturbation theory the optical absorption caused by the simultaneous creation of a Wannier exciton and a LO phonon. In insulators with $E_B \gg \hbar\omega_l$, a striking exhibition of quantum-mechanical interference is predicted for $\hbar\omega \approx E_{xm}$. Excepting for this interference effect, there are no sharp phonon peaks in the alkali halides if one assumes a linear exciton-phonon interaction. Peaks are predicted, but they are extremely broad and $\hbar\omega_l$ can be placed energetically as a function of \vec{k} anywhere in the Brillouin zone for $\hbar\omega > E_{xm} + \hbar\omega_l$, by using presently available experimental and theoretical parameters.

I. INTRODUCTION

This paper presents an illustration of the quantum-mechanical interference effect found in excitonic transitions. The particular transition of interest is that of the absorption of a photon by an exciton with the simultaneous creation of an LO phonon. Since the process is a second-order one, the measurable effect in absorption is expected to be small and can, therefore, be said to be in the domain of fine structure. In conjunction with this, the effect has not previously been predicted, so that this may be a reason why it has not yet been reported as observed experimentally.

Segall¹ and Segall and Mahan² have considered the

case for phonon-assisted emission, which is closely related to the absorption process. The threshold for emission is $E_{x1} - \hbar\omega_l$, whereas, for absorption, it is $E_{x1} + \hbar\omega_l$, which takes us into the thick of the exciton bands. For this reason, the excitonic intermediate states assume special importance in the following work. Another difference in approach is that their treatment was for semiconductors, where typically $E_B < \hbar\omega_l$. For our case, choosing $E_B \gg \hbar\omega_l$, facilitates a much cleaner theory to study the phonon effects. For this reason, we choose to apply our results to the alkali halides, and KI in particular, since E_B is less than the spin-orbit splitting, which again lends to a less complicated treatment. Another supporting feature of KI is the wealth of ex-